Electronic Supplementary Material (ESI) for Journal of Materials Chemistry A.

Supporting Information

Fast, simultaneous metal reduction/ deposition on electrospun a-WO_3/PAN nanofiber membranes and their potential applications for water purification and noble metal recovery

Jing Wei[†], *Xiuling Jiao*[†], *Ting Wang**[†], *Dairong Chen**[†]

[†]*School of Chemistry & Chemical Engineering, Shandong University; National Engineering Research Center for Colloidal Materials, Shandong University, Jinan 250100, P. R. China.*

Experimental section

1. Materials

All chemicals were of analytical grade and used as received without further purification. Tungsten hexachloride (WCl_6, 99.9%) was purchased from Shanghai Macklin Biochemical. Polyvinylpyrrolidone (PVP), polyacrylonitrile (PAN) were purchased from Bodi Chemical Limited Company of Tianjin. Chloroauric acid ($HAuCl_4$), chloroplatinic acid (H_2PtCl_6) and potassium tetrachloropalladate (K_2PdCl_4) were purchased from Sinopharm Chemical Reagent. Silver nitrate ($AgNO_3$) was purchased from Xilong Chemical Co. Ltd.. Cupric chloride dehydrate ($CuCl_2 \cdot 2H_2O$), mercuric chloride ($HgCl_2$), lead dinitrate ($Pb(NO_3)_2$) and potassium dichromate ($K_2Cr_2O_7$) were purchased from Sinopharm Chemical Reagent. Absolute ethanol (99.9%) and N, N-dimethylformamide (DMF) were purchased from Sinopharm Chemical Reagent. All the ion standard solutions (1000 μg/ml) were purchased from Shanghai Macklin Biochemical.

2. Characterization

The field emission scanning electron microscopy (FE-SEM SU8010) was used to record the morphology and elemental composition of the membranes. The sample was first sputtered with 1 nm Au layer using a sputter equipment to avoid the electron charging effect. The scanning transmission electron microscope (HAADF-STEM) images and the EDS mapping images of the nanofibers were collected by Talos F200X operated at 200 kV. Optical photographs were recorded by a Leica digital camera. Powder X-ray diffraction (XRD) patterns were gathered on a Rigaku D/Max 2200pc diffractometer equipped with graphite monochromatized Cu K_α radiation (λ = 0.15418 nm). The Fourier transform infrared (FT-IR) spectroscopy was measured by a Bruker Alpha spectrometer using KBr pellet in the range 400-4000 cm^{-1}. The Raman spectra were measured with a micro-Raman LabRAM HR800 spectrometer. The diffuse reflectance data were measured using a UV-Vis Spectrophotometer (Cary 100) with $BaSO_4$ as reference. Thermo Ultimate 3000 attached Thermo LCQ Fleet (HPLC-MS) was carried out to determine the composition of the membranes. Thermogravimetric (TGA) measurements were recorded on a STA449 F3 Jupiter(NETZSCH) analyzer in air with a heating rate of 5°C min^{-1}. X-ray photoelectron spectroscopy (XPS) was performed on a Perkin-Elmer PHI-5300 ESCA instrument with a Mg K_α ADES (h=1253.6 eV) source at a residual gas pressure below 10^{-8} Pa. Electrochemical measurements (cyclic voltammetry) were performed on a CHI760E electrochemical workstation with a three-electrode setup and 1M WCl_6/DMF as the electrolyte.

3. Membrane fabrication

For the preparation of the a-WO_3/PAN membranes, 0.5 g PAN were dissolved in 6.0 mL DMF to form a transparent solution. Various amounts of WCl_6 were added into the polymer solutions with vigorous stirring. The reaction was in ambient conditions, the oxygen in air and residual water in DMF helps oxidation and hydration of the WCl_6 precursors. In the first 3 minutes, there were white smokes which are HCl gas continuously come out. Within 5-7 min, the solution change from colorless to jacinth and finally to a blue color owing to the formation of a large amount of small a-WO_3 clusters. After reaction for 5 min and 15 min, we took some samples out and measured the samples using the mass spectroscopy (MS, Figure SS1). The MS spectra show that after 5 min, there is a peak with m/z value of 704, indicates existence of large amounts of $H_2W_6O_{19}$ clusters. After 15 min, the MS spectrum shows a series of peaks, indicating the formation of a-WO_3 clusters with different sizes. The UV−vis spectra (Figure SS2) of the precursor solution indicate that the solution exhibited reversible color switch from colorless to blue upon UV irradiation. The UV-vis spectra indicate the precursor absorption edge is near 300 nm, which also proves the precursors are small a-WO_3 clusters. After reaction for 15-20 min, we obtain a colloidal, viscous solution of the a-WO_3 and PAN without any noticeable precipitates.

Then, as-prepared viscous solution was loaded into 10 mL plastic syringe equipped with a needle of 0.7 mm diameter. The flow rate of the syringe pump was 0.7 mL/h and the distance between the collector and the needle was 20.0 cm. The applied voltage was held at 20 kV. The humidity was kept at 20±5 %. The electrospun fibrous membranes were ripped down from the aluminum foil and vacuum-dried at 80 °C for 24 h to remove the DMF and other volatile residuals, this long time drying also promotes the connection of the WO_3 clusters and formation of the a-WO_3 network. As-obtained membranes were light yellow color and ready for further characterization.

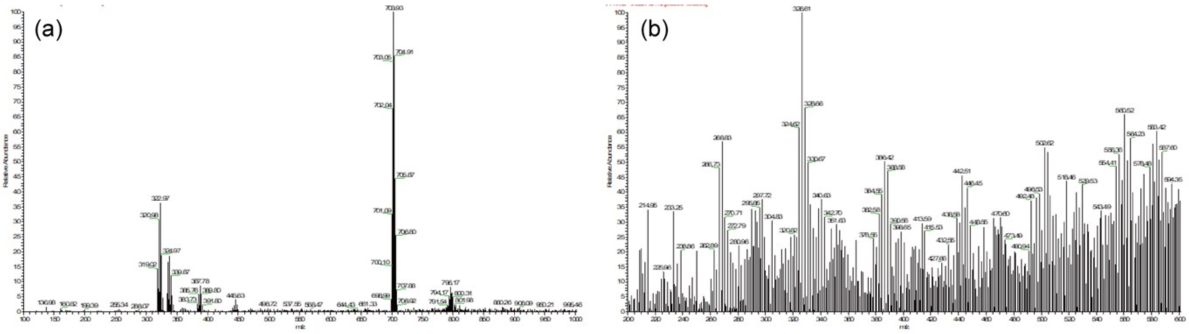

Figure SS1. MS spectra of the precursor solution after reaction for (a) 5 min and (b) 15 min.

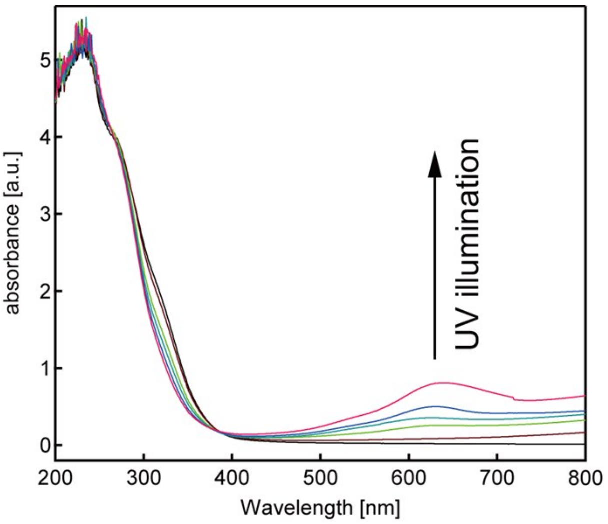

Figure SS2. A series of UV-vis spectra for the precursor a-WO_3 upon UV illumination.

4. Metal removal/recovery from wastewater

The concentrations of various metal ion during all the experiments were detected by inductively coupled plasma-mass spectrometry (iCAP-RQ ICP-MS). The aqueous solutions of various ions (Ag^+, $AuCl_4^-$, $PtCl_6^{2-}$, $PdCl_4^{2-}$, Hg^{2+}, Pb^{2+}, Cu^{2+}, Cr^{6+}) were obtained by diluting the standard solution of the metal precursors with proper amounts of super cleaning water. The solutions were all deaerated using N_2 gas bubbling into the precursor solution for 10-15 min. When the experiments were in a beaker, a plastic film was coated on the beaker to avoid air contact with the solution. There would still be some air in the solution, however, a small amount of oxygen does not influence the experiments.

5. Recycling the noble metal nanoparticles

For noble metal recycling, the soluble metal pollutants deposited on the membrane were first removed by immersing the membrane in acidic water. Then the nanofiber membrane can be dissolved by immersing them in 20 mL DMF with sonication for about 20 min. As-obtained cloudy suspension was centrifuged at 3000 rpm for 10 min. The noble metal precipitates obtained were further washed using 20 mL of 1 M NH_4OH to remove the surface attached a-WO_3 clusters, the as-obtained noble metal nanoparticles were dried in an oven at 200 °C for 24 h for further characterizations.

Supplementary figures:

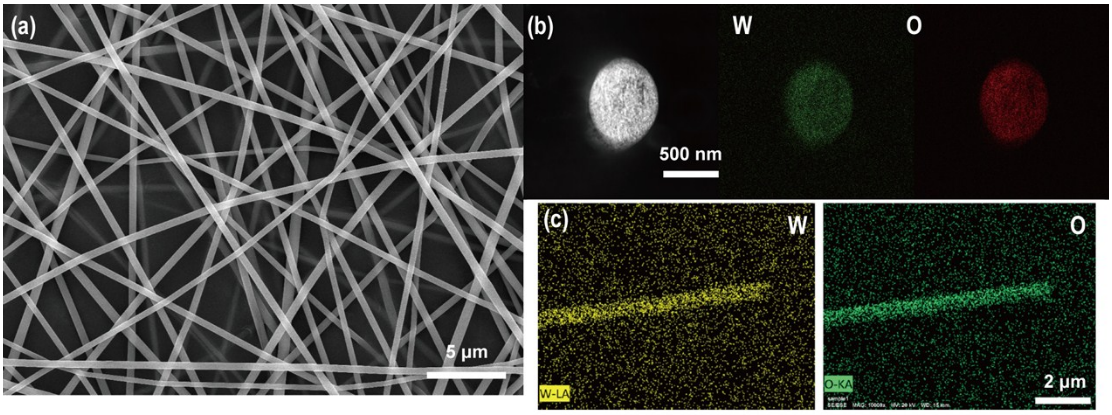

Figure S1. (a) SEM image of the nanofiber membrane with 60 wt% a-WO_3 contents. The elemental mapping images of the nanofiber show (b) the cross section and (c) the side view of the distribution of the W and O elements.

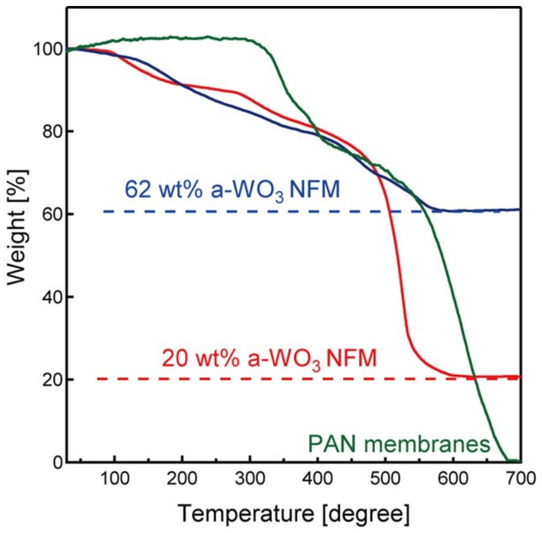

Figure S2. TGA results confirming the contents of the a-WO_3 in the nanofiber membranes.

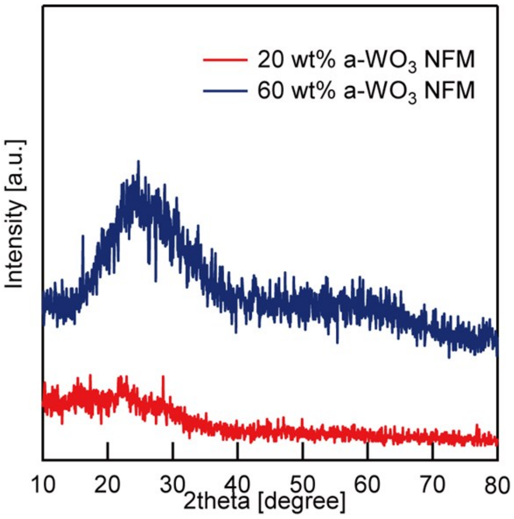

Figure S3. XRD patterns of the nanofiber membranes with 20 wt% and 62 wt% a-WO_3, showing both nanofibers are amorphous.

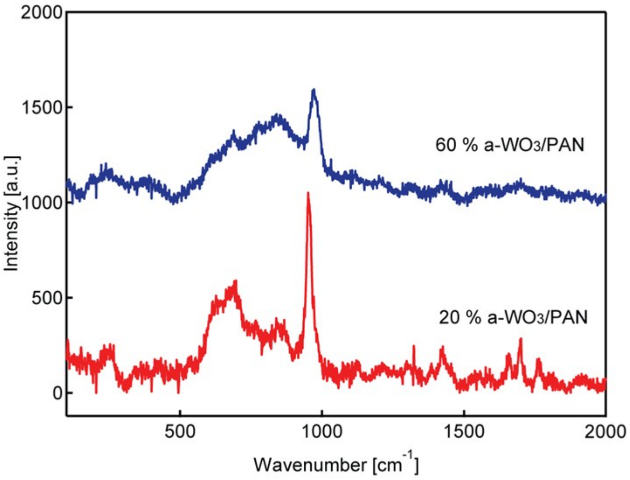

Figure S4. Raman spectroscopy results of the nanofiber membranes showing the increasing degree of connectivity with increased a-WO_3 contents.

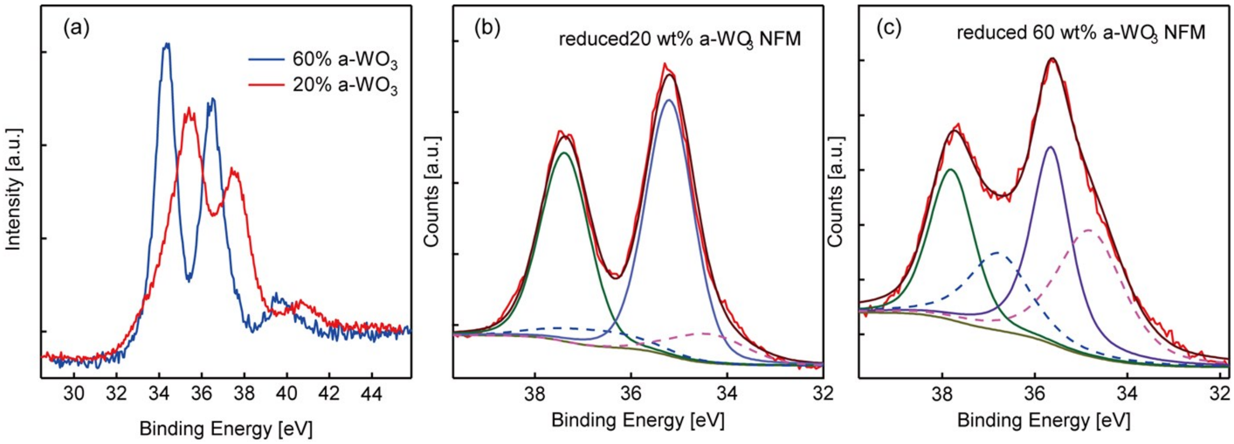

Figure S5. XPS spectra of the light yellow and photo-reduced a-WO_3/PAN composite membrane with 20 % and 62 % a-WO_3 incorporation. (a) XPS spectra of the light-yellow membranes with 20 wt% (blue) and 62 wt% (red) a-WO_3 contents. (b,c) XPS results for W of the photo-reduced membrane with 20 wt% and 62 wt% a-WO_3. The red curves are the original data and the black curves are the fitting lines. The dashed lines are fitting curves for W^{5+} and the colored solid lines are for W^{6+}.

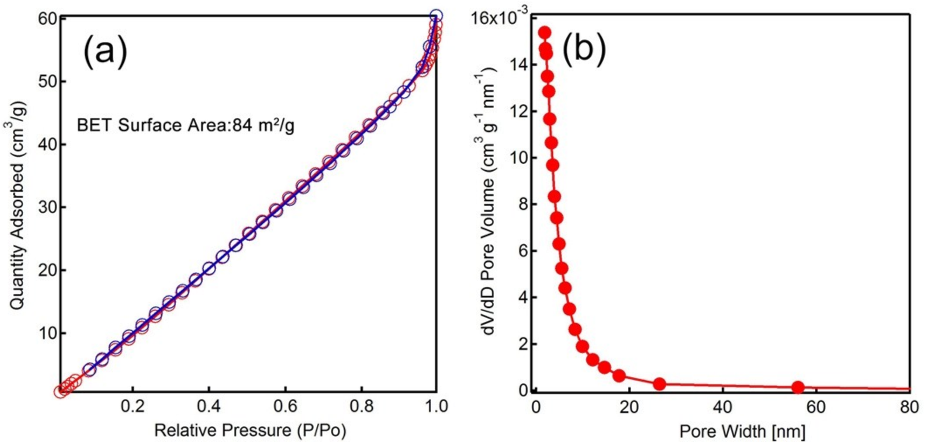

Figure S6. (a) N_2 sorption isotherms measured at 77 K of the nanofiber membranes with 62 wt% a-WO_3 contents. (b) The pore-size distribution calculated using the BJH method.

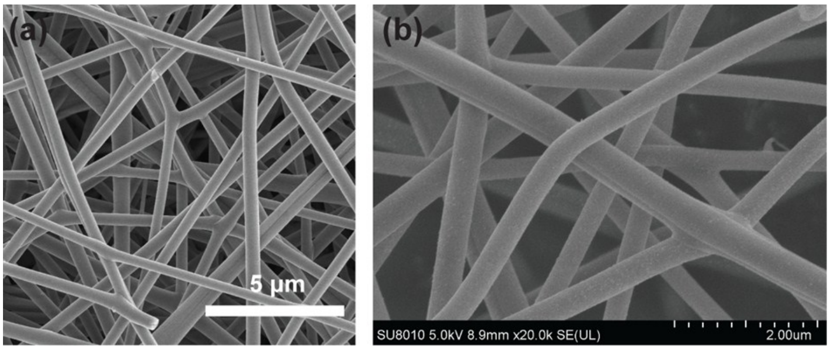

Figure S7. The SEM images showing the morphologies of the 62 wt% a-WO_3 membrane (a) before and (b) after immersing in water for 2 days.

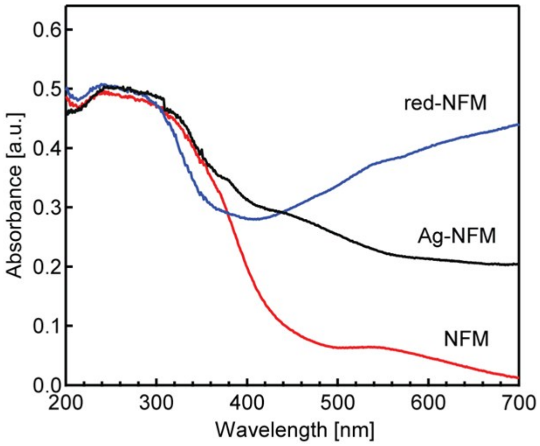

Figure S8. UV-vis spectra showing the absorption of the a-WO_3/PAN nanofiber membrane before solar light illumination (red), after solar light illumination (blue), and after Ag deposition (black).

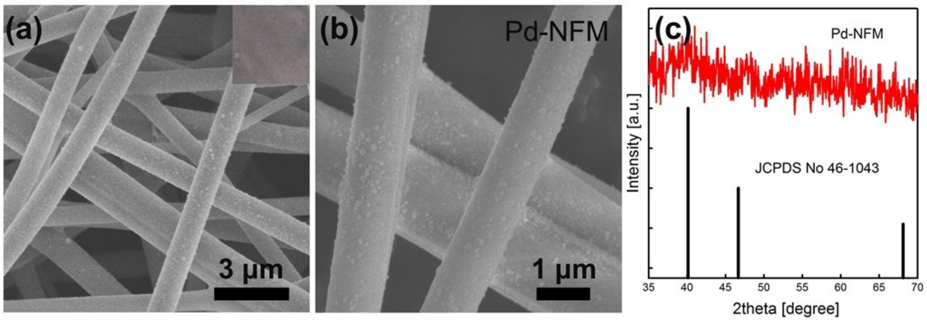

Figure S9. SEM images and XRD patterns of the nanofiber membrane after deposited with Pd nanoparticles.

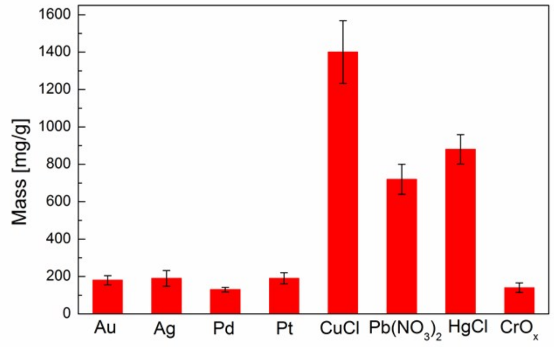

Figure S10. Saturated capacities of the membrane when deposited with different metal compounds.

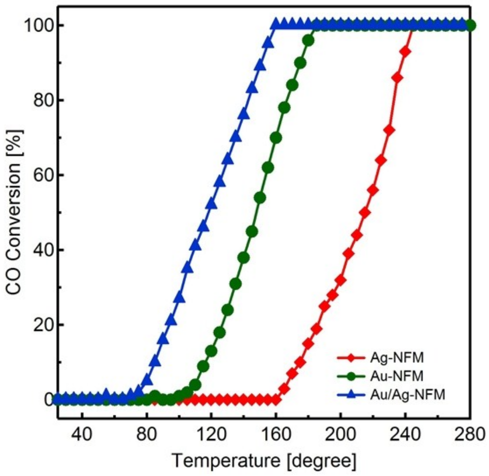

Figure S11. The noble metal coated nanofiber membranes as catalysts for CO oxidation reactions.

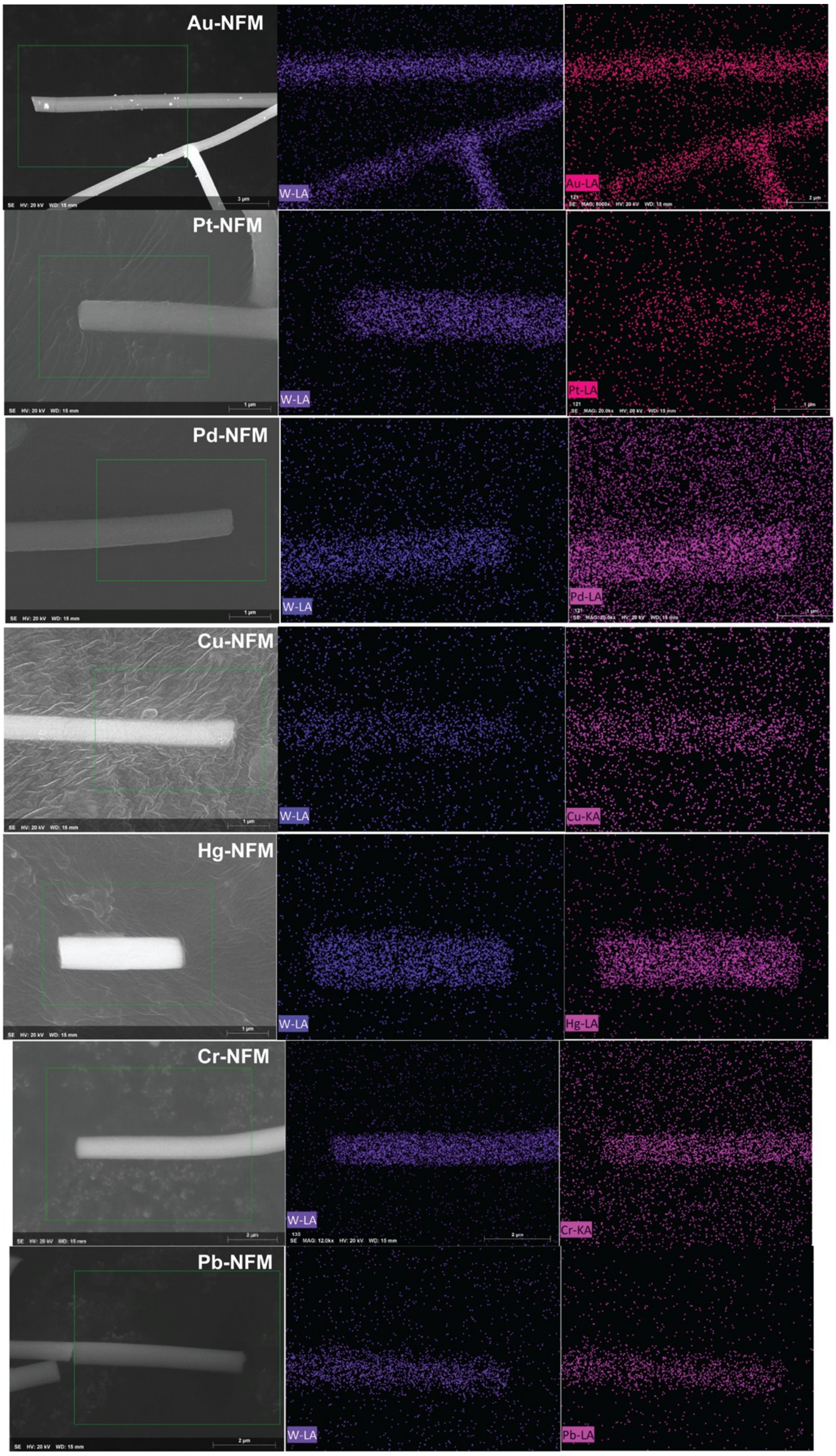

Figure S12. SEM images and the corresponding elemental mapping for W element in the NFM and the deposited metals. (a) Ag, (b) Au, (c) Pt, (d) Pd, (e) Cu, (f) Hg, (g) Cr, (h) Pb.

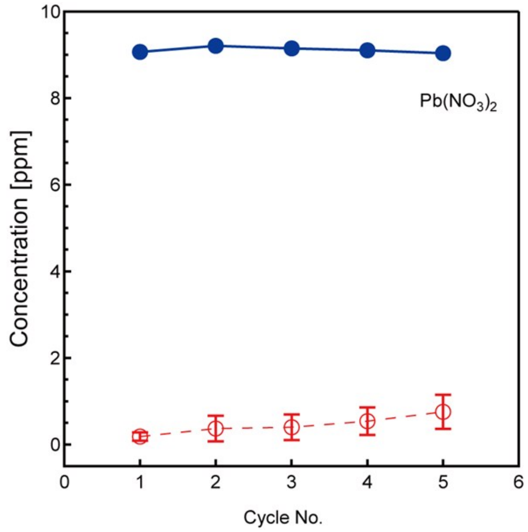

Figure S13. Pb^{2+} concentration of lead-polluted water before and after purified by the same NFM for 5 cycles. Before each cycle, the membrane was regenerated by mild washing with acidic water.

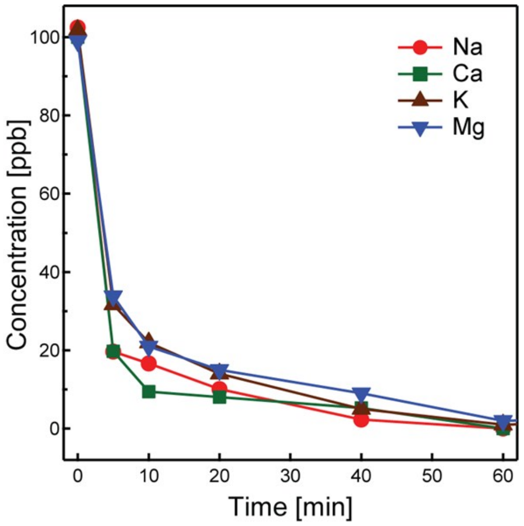

Figure S14. Metal removal/recovery in ppb level for $AgNO_3$ in the presence of irreducible Na^+, K^+, Ca^{2+}, Mg^{2+} ions.

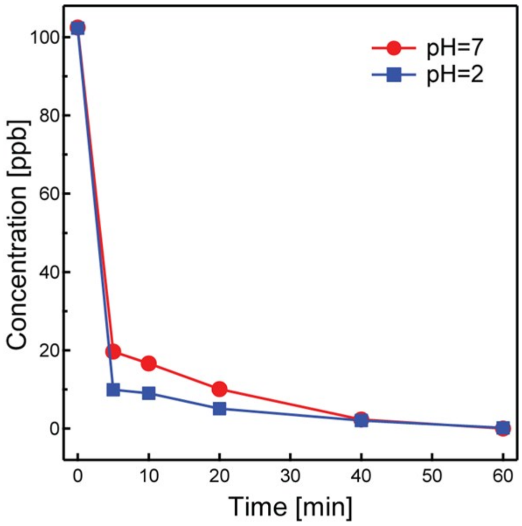

Figure S15. A comparison of the metal removal kinetics under pH value of 2 and 7.

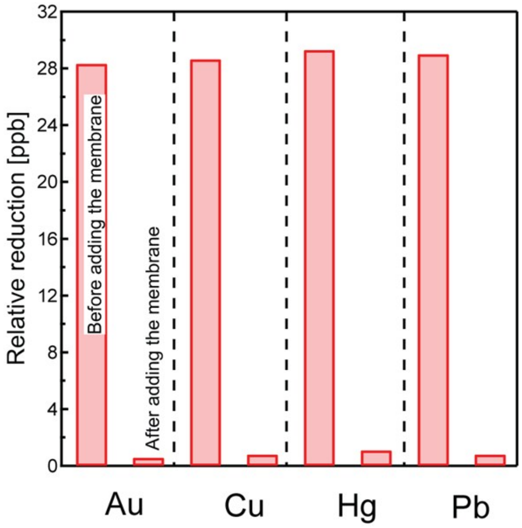

Figure S16. Simultaneous removal/recovery of four types of metals in wastewater in 100 ppb and the comparison of the metal concentration before and after immersing 0.1 g NFM in 1 L of the wastewater for 1 h.

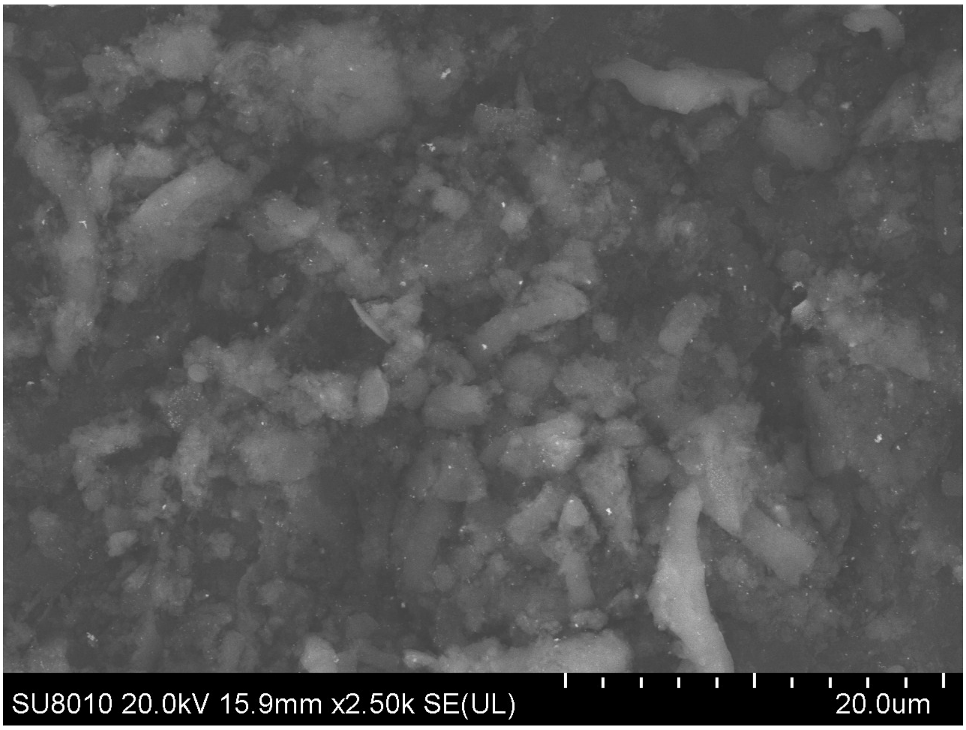

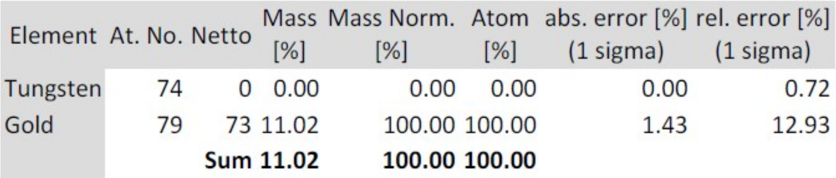

Element	At. No.	Netto	Mass [%]	Mass Norm. [%]	Atom [%]	abs. error [%] (1 sigma)	rel. error [%] (1 sigma)
Tungsten	74	0	0.00	0.00	0.00	0.00	0.72
Gold	79	73	11.02	100.00	100.00	1.43	12.93
		Sum	**11.02**	**100.00**	**100.00**		

Figure S17. SEM images of the recycled Au nanoparticles and the elemental analysis showing their high purity, there are no a-WO_3 attached on the Au nanoparticle surfaces.

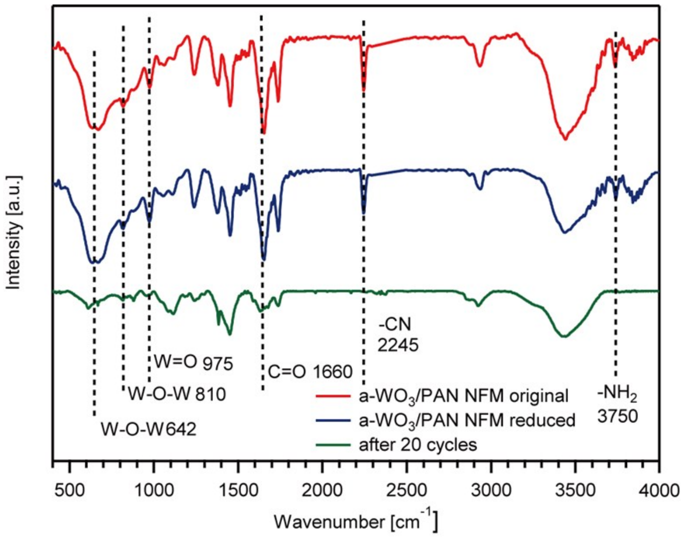

Figure S18. IR spectra of the original membrane, the photo-reduced a-WO_3/PAN hybrid membrane and the membrane after 20 reduction-oxidization cycles.

The sharp peak at 2245 cm^{-1} can be assigned to the vibration of the nitrile groups (-CN) in the side chain of PAN, which almost disappeared after 20 reduction-oxidization cycles, meaning the -CN groups are consumed in the reduction-oxidization reactions. In the IR spectrum of the initial NFM, there are also peaks at 1660 cm^{-1} which can be assigned to the vibrations of the

C=O bonds and peaks at 3750cm^{-1}, which can be assigned to the -NH_2 vibrations. Parts of the -CN groups are hydrated in the NFM and transfer to -$CONH_2$ groups. These acylamides can work effectively as electron donors and proton donors for the reduction of the NFM.

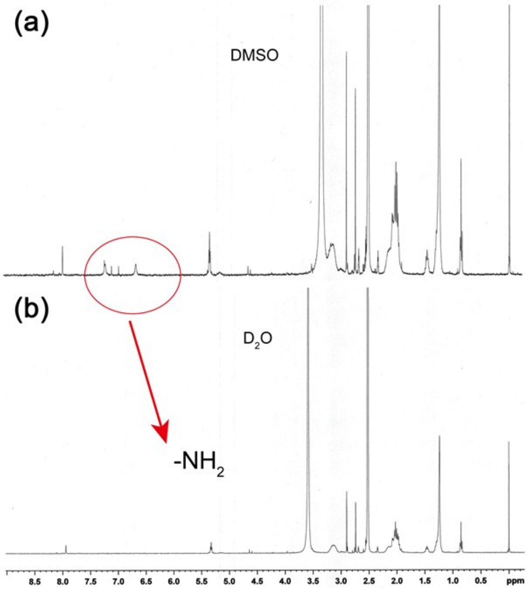

Figure S19. 1H NMR spectra of the nanofiber membrane dissolved in (a) DMSO and (b) D_2O.

In the 1H NMR results, protons on N typically have wide ranges of expected chemical shifts, as shown in Figure S16. The peaks with chemical shifts from 6.5-7.5 ppm can be identified as the NH_2 groups in the PAN matrix. Because these protons are acidic and exchangeable, with a protic deuterated solvent, such as D_2O, the NH_2 protons will exchange with the deuterium and the peaks will shrink or disappear entirely. We switched the solvent from DMSO to D_2O and observed the disappearance of the peaks from 6.5-7.5 ppm, this observation further confirms the peaks from 6.5-7.5 ppm were active protons from the NH_2 groups.

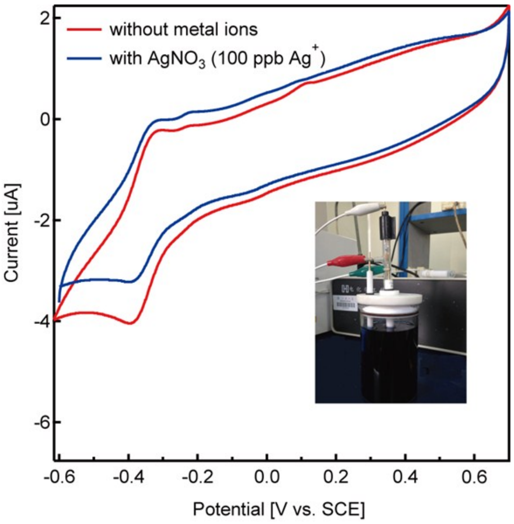

Figure S20. Cyclic voltammograms curve of the suspended small a-WO_3 clusters in water (a) without any metal ions and (b) with 100 ppb of Ag^+.

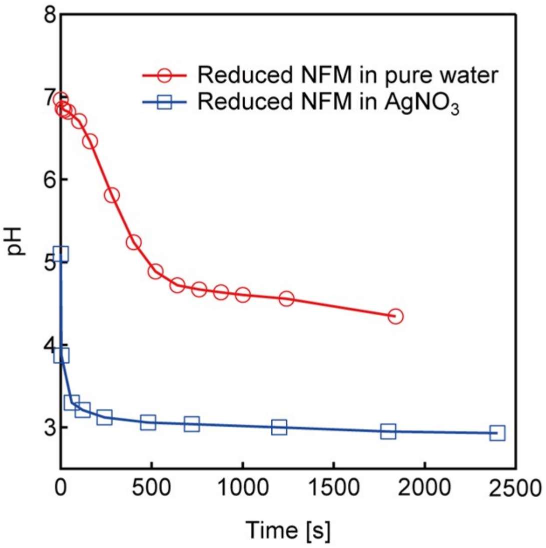

Figure S21. The pH values changing with time after immersing a 0.03 g reduced NFM in 25 mL $AgNO_3$ (0.1 M) and in 25 mL pure water.

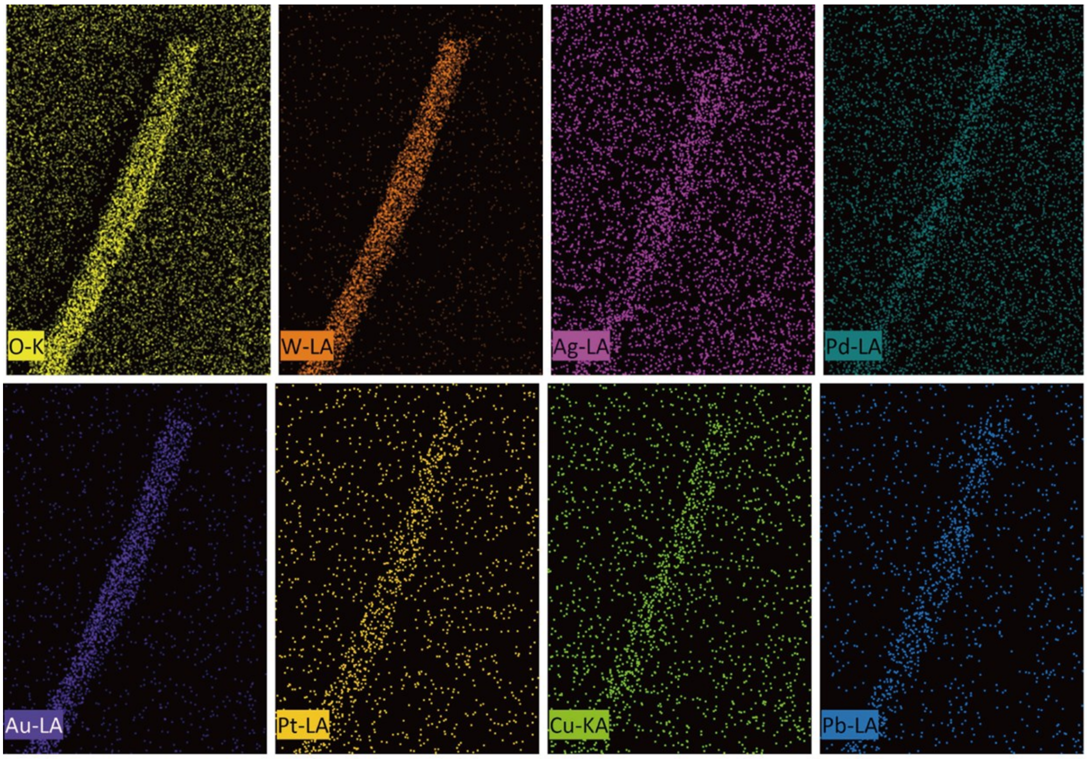

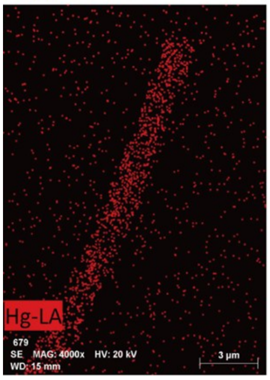

Element	Ag	Pd	Au	Pt	Cu	Pb	Hg
Atom [%]-5 min	22.53	0.89	0.74	0.77	0.66	1.46	0.16
Atom [%]-60 min	3.6	3.32	4.62	3.73	1.04	9.7	1.01

Figure S22. Elemental mapping images from SEM showing the homogenous distribution of the W, O elements and the deposited Ag, Pd, Au, Pt, Cu, Pb and Hg elements after immersing the membrane in water containing various metals for 30 min. The table shows the relative contents of the deposited metals after immersing the membrane for 5 min and 30 min.

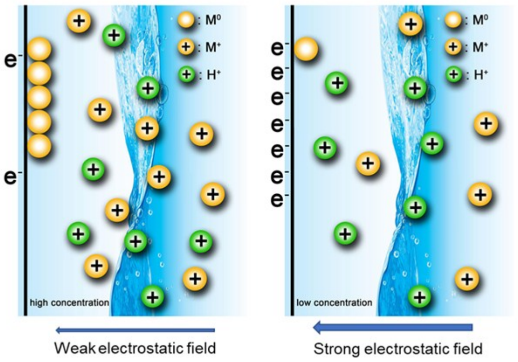

Figure S23. Schematic illustration of the ppb level metal removal/recovery mechanism. The left part shows when metal concentration is high, nanofiber surface is only slightly charged and there is a weak electrostatic field. When metal concentration is low, while the protons diffuse into the electrolytes, there are no enough metal ions to be reduced on the nanofiber surface, then more and more electrons accumulate on the nanofiber surfaces. The nanofibers are negatively charged and induce a strong electrostatic field.

Table S1. Metal pollutant removal properties of the NFM using WHO standard as a reference.

	Metal concentration after purification	Values listed in the WHO guideline
Cu	0.53 ppb	2 ppm
Ag	0.18 ppb	2 ppb
Hg	1.1 ppb	6 ppb
Cr	6.9 ppb	50 ppb
Pb	1.41 ppb	10 ppb